

ν is the Poisson's ratio, and the parameter κ is defined as

$$\begin{aligned} \kappa &= 1 \quad \text{if} \quad \sigma_e = \sigma_{e_{\max}} \quad \text{and} \quad d\sigma_e \geq 0 \\ \kappa &= 0 \quad \text{if} \quad \sigma_e < \sigma_{e_{\max}} \quad \text{or if} \quad \sigma_e = \sigma_{e_{\max}} \quad \text{and} \quad d\sigma_e < 0 \end{aligned} \quad (\text{A5})$$

The static equilibrium equations are

$$\sigma_{11} = \sigma_{22} = \rho r / 2h \quad \text{and} \quad \sigma_{33} = 0 \quad (\text{A6})$$

Acknowledgment

The authors would like to thank Dr. J. Ari-Gur and R. D. Richard for helpful suggestions on this work. This work is part of a doctoral thesis by the first author that is to be submitted to the Senate of Technion—Israel Institute of Technology.

References

- ¹Hoff, N.J., "Dynamic Stability of Structures," *Dynamic Stability of Structures*, edited by G. Herman, Pergamon Press, New York, 1967.
- ²Vyrlan, P.M. and Shil'krut, D.L., "Stability of Equilibrium Forms of Geometrically Nonlinear Spherical Shells," *Izvestiya Akademii Nauk SSSR, Mekhanika Tverdogo Tela*, Vol. 13, No. 4, 1978, pp. 170-176.
- ³Ginsburg, S. and Gellert, M., "Numerical Solution of Static and Dynamic Nonlinear Multi-Degree-of-Freedom Systems," *Computer Methods in Applied Mechanics and Engineering*, Vol. 23, 1980, pp. 111-125.
- ⁴Durban, D. and Baruch, M., "Elastic-Plastic Behavior of a Spherical Membrane under Internal Pressure," *Israel Journal of Technology*, Vol. 12, 1974, pp. 23-30.
- ⁵Gear, C.W., *Numerical Initial Value Problems in Ordinary Differential Equations*, Prentice-Hall, Englewood Cliffs, NJ, 1971.

Buckling of Composite Plates Using Shear Deformable Finite Elements

Frank Kozma*

LTV Corporation, Dallas, Texas
and

Ozden O. Ochoa†
Texas A&M University, College Station, Texas

Introduction

THE instability problem of a composite plate is more complicated than that of an isotropic plate due to the orthotropic properties of each lamina. The focus of this Note is the utilization of a recently developed shear deformable, composite plate element, QHD40, within a finite element program to solve for the critical buckling loads.^{1,2} The effort is noteworthy in that the displacement field used in formulation of the composite plate element contains higher-order terms. This allows a more refined model for the stress distribution within the structure, a progression of previous work relating to shear deformation in isotropic and anisotropic plate structures.²⁻⁵ Ochoa et al.¹ presented the results of the eigen-

value problem for the vibration of composite plates using this element. Herein the critical buckling loads for composite plates are calculated and compared to currently available numerical finite element methods (FEM) and analytical results with various fiber orientations and boundary support conditions.⁶⁻⁸

Stability Problem

The stability problem can be formulated in a manner analogous to the standard eigenvalue problem. This can be expressed in matrix notation as

$$([K]\{u\} = -\lambda[KG]\{u\} \quad (1)$$

where $[K]$, λ , $[KG]$, and $\{u\}$ are the stiffness matrix, the lowest eigenvalue (loading), the geometric or initial stiffness matrix, and the eigenvector of nodal displacements corresponding to an eigenvalue, respectively. The solution procedure for Eq. (1) can be summarized as follows:

- 1) Evaluate stiffness matrix $[K]$ for the chosen element

$$[K] = \int_{\text{vol}} [B]^T [D] [B] dV \quad (2)$$

- 2) Solve for displacements $\{u\}$ by decomposition and back substitution and calculate the stresses.

- 3) Evaluate the geometric stiffness matrix $[KG]$.

After formulation of the geometric stiffness matrix, the lowest eigenvalue is solved for by the inverse iteration method. Having solved for $\{u_{i+1}\}$ by back substitution, $\{u_{i+1}\}$ is normalized to $\{un_{i+1}\}$, where

$$\{un_{i+1}\} = \{u_{i+1}\} / \lambda_{i+1} \quad (3)$$

The test for convergence is stated as

$$|(\lambda_{un_{i+1}} - \lambda_{un_i})| < e \quad (4)$$

where e is a prescribed value. After convergence, λ_i is obtained by taking the inverse of the value used to normalize $\{u_i\}$. For comparison with previously published results, the following nomenclature is introduced:

$$N_x = \lambda_i / B \quad (5)$$

where N_x and B are the critical buckling load per unit length and width of the plate, respectively.

Element Description

QHD40 is an eight noded quadrilateral plate element with seven degrees of freedom at each corner node and three degrees of freedom per midside node for use in linear/nonlinear applications. The element and associated finite element routines were developed by Engblom and Ochoa.^{1,2} The assumed displacement field of the element is

$$\begin{aligned} u(x, y, z) &= u_0(x, y) + z\Psi_x(x, y) + z^2\phi_x(x, y) \\ v(x, y, z) &= v_0(x, y) + z\Psi_y(x, y) + z^2\phi_y(x, y) \\ w(x, y, z) &= w_0(x, y) \end{aligned} \quad (6)$$

The neutral surface displacements are represented by u_0 , v_0 , and w_0 , the rotation about the y axis is given by Ψ_x , and the rotation about the x axis is denoted by Ψ_y . Coefficients of z^2 , ϕ_x , and ϕ_y can be interpreted as contributions from transverse deformations. In-plane displacements (u_0 , v_0) and the higher-order terms (ϕ_x , ϕ_y) are expanded in bilinear form as

$$[1 \ x \ y \ xy] \{\alpha\} \quad (7)$$

Received March 27, 1985; revision received Feb. 20, 1986. Copyright © American Institute of Aeronautics and Astronautics, Inc., 1986. All rights reserved.

*Structures Engineer, Structural Technology Group, Vought Aero Products Division.

†Assistant Professor, Department of Mechanical Engineering. Member AIAA.

The transverse displacement w_0 and the independent rotations Ψ_x and Ψ_y are expanded as

$$[1 \ x \ y \ x^2 \ xy \ y^2 \ x^3 \ y^3] \{\beta\} \quad (8)$$

Finally, the stress field associated with this element has the following distribution: From constitutive equations,

$$\sigma_{xx} = \ell(z^2, x^2, y^2), \sigma_{yy} = \ell(z^2, x^2, y^2), \sigma_{xy} = \ell(z^2, x^2, y^2) \quad (9)$$

and from equilibrium calculations,

$$\sigma_{xz} = \ell(z^3, x, y), \sigma_{yz} = \ell(z^3, x, y), \sigma_{zz} = \ell(z^3) \quad (10)$$

Model Description

A quarter of a square plate of 16 elements is modeled for the eigenvalue analysis problem of symmetric laminates. The thicknesses of elements are changed to study the effects of the

Table 1 Material elastic moduli used for test cases, psi

Material	E_1	E_2	G_{12}, G_{13}	G_{23}	ν_{12}, ν_{13}
1	40,000,000	1,000,000	600,000	500,000	0.25
2	6,333,333	1,000,000	666,700	500,000	0.20

Table 2 Material anisotropy effect on buckling loads of $[0^\circ/90^\circ/90^\circ/0^\circ]$ square plates ($B/t=10$, material 1)

E_1/E_2	CPT	HSDT (Ref. 6)	Three-dimensional (Ref. 7)	QHD40
3	5.7538	5.1143	5.2944	5.2914 (5.2914) ^a
10	11.492	9.774	9.7621	9.7931
20	19.712	15.298	15.0191	15.205
30	27.936	19.957	19.3040	19.7081
40	36.160	23.340	22.8807	23.5406 (23.6713) ^a

^aQHD40 without higher order terms.

Table 3 Buckling loads $\lambda_b = P_{x0}B^2/(E_2t^3)$ of $[45^\circ/-45^\circ]_s$ symmetric angle-ply square plates

B/t	Ref. 6	QHD40	QHD40 w/o terms
a) With simply supported boundary conditions (material 1)			
10	21.125	24.991	24.636
20	29.150	32.468	32.205
50	34.596	37.114	37.055
100	36.645	39.478	39.461
b) With clamped boundary conditions (material 1)			
10	31.0778	36.054	35.6700
100	113.431	101.188	101.044

Table 4 Buckling loads $\lambda_b = P_{x0}B^2/(E_2t^3)$ of a $[0^\circ/+45^\circ/90^\circ]_s$ square plates

B/t	Ref. 6	QHD40	QHD40 w/o terms
a) With simply supported boundary conditions (material 1)			
10	26.799	26.974	28.051
20	37.115	37.205	37.651
50	41.877	41.957	42.042
100	42.819	42.983	43.004
b) With clamped boundary conditions (material 1)			
10	39.7451	43.175	43.9406
100	135.725	129.863	130.338

aspect ratio B/t . The boundary conditions utilized are simply supported/simply supported, simply supported/clamped, and clamped/clamped. Cases with and without the higher-ordered terms of the displacement functions are also studied.

For nonsymmetrical laminates, a full square plate model of 16 elements is utilized. Boundary conditions for all cases on nonsymmetrical layups are either simply supported/simply or simply supported/clamped with no prescribed conditions on the higher-order terms. Material moduli used are listed in Table 1.

Results and Summary

Solutions of the critical load problem of composite plate models formulated with the QHD40 element are displayed in Tables 2-5. Table 2 is a comparison of a simply supported composite plate $[0^\circ/90^\circ/90^\circ/0^\circ]$ with varying E_1/E_2 ratios. The results are compared to those obtained by the classical plate theory (CPT), higher-order shear deformation theory (HSDT) obtained by Phan and Reddy⁶ and the three-dimensional elasticity theory obtained by Noor.⁷ Table 3a presents buckling loads for the simply supported case of a symmetric angle ply $[45^\circ/-45^\circ]_s$ composite plate. Results for the clamped/clamped case are as shown in Table 3b. The data provided in Table 4a is for a symmetric angle ply $[0^\circ/\pm 45^\circ/90^\circ]_s$ composite plate. The loads obtained are consistent with those obtained by Phan and Reddy.⁶ For clamped boundary conditions of the same plate, the results are shown in Table 4b. Table 5 displays buckling loads for antisymmetric $[0^\circ/90^\circ]$ and $[0^\circ/90^\circ/0^\circ/90^\circ/0^\circ/90^\circ]$ cross-

Table 5 Buckling loads $\lambda_b = P_{x0}B^2/(E_2t^3)$ of $[0^\circ/90^\circ/0^\circ/90^\circ/0^\circ/90^\circ]$ antisymmetric cross-ply square plates with simply supported boundary conditions ($B/t=10$, material 1)

E_1/E_2	Plys	QHD40	Ref. 7
10	2	6.3242	6.1181
20	2	8.2420	7.8196
40	2	11.5778	10.8167
10	6	9.7923	9.6051
20	6	15.5365	15.0014
40	6	25.1025 (25.4425) ^a	23.6689

^aQHD40 without higher-order terms.

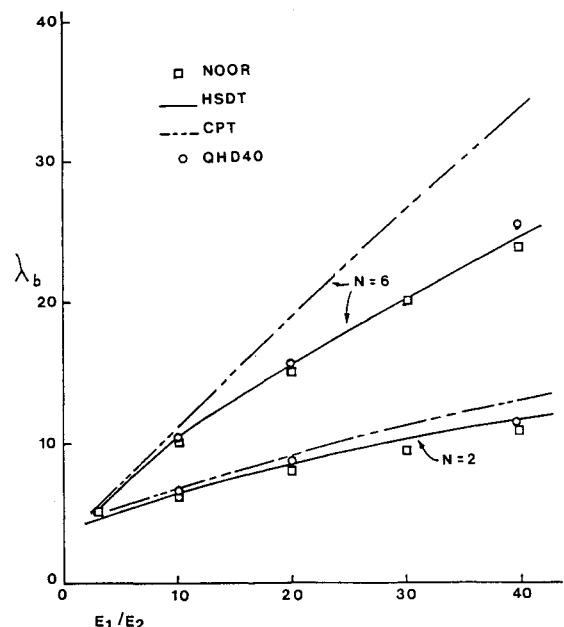


Fig. 1 Effect of material anisotropy on the buckling of $[0^\circ/90^\circ/\dots]$ antisymmetric cross-ply square plates ($B/t=10$, n =number of layers of $0^\circ/90^\circ$).

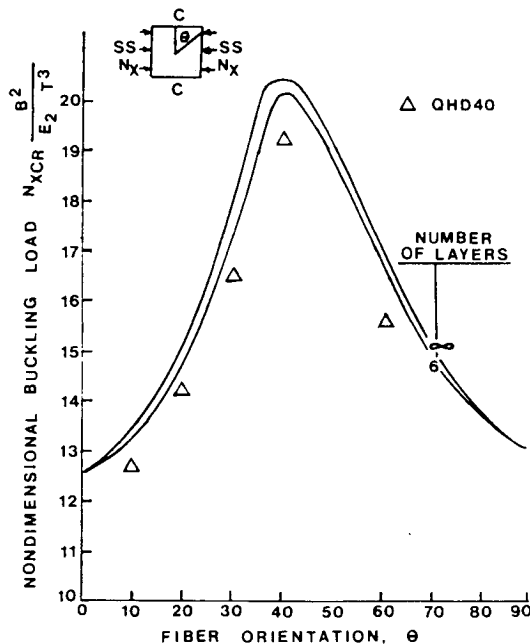


Fig. 2 Display of critical buckling loads for antisymmetric angle-ply square plate vs ply orientation with simply supported/clamped boundary conditions (material 2).

ply composite plates. For these cases, the E_1/E_2 ratio is varied while the aspect ratio is held constant. The results are in good agreement to those obtained by Noor⁷ as shown in Fig. 1.

Figure 2 displays buckling loads of antisymmetric angle-ply plates with simply supported/clamped boundary conditions for different ply orientation angles θ . These are compared to those obtained by Sharma.⁸ As can be observed, the present formulation yields an upper bound to the elasticity model. However, the overall results are good and the formulation is much less cumbersome than a three-dimensional approach.

References

- ¹Ochoa, O.O., Engblom, J.J., and Tucker, R., "A Study of the Effects of Kinematic and Material Characteristics on the Fundamental Frequency Calculations of Composite Plates," *Journal of Sound and Vibration*, Vol. 101, No. 2, 1985, pp. 141-148.
- ²Engblom, J.J. and Ochoa, O.O., "Thru-the-Thickness Stress Predictions for Advanced Composite Material Configurations," AIAA Paper 84-0859, 1984.
- ³Mindlin, R.D., "Influence of Rotary Inertia and Shear on Flexural Motions of Isotropic, Elastic Plates," *Journal of Applied Mechanics*, Vol. 18, 1951, pp. 31-38.
- ⁴Whitney, J.M. and Pagano, N.J., "Shear Deformation in Heterogeneous Anisotropic Plates," *Journal of Applied Mechanics*, Vol. 37, No. 4, 1970, pp. 1031-1036.
- ⁵Dong, S.B. and Tso, F.K., "On a Laminated Orthotropic Shell Theory Including Transverse Shear Deformation," *Journal of Applied Mechanics*, Vol. 39, No. 4, Dec. 1972, pp. 1091-1097.
- ⁶Phan, N.D. and Reddy, J.N., "Analysis of Laminated Composite Plates Using a Higher-Order Shear Deformation Theory," *International Journal for Numerical Methods in Engineering*, Vol. 21, No. 12, 1985, pp. 2201-2219.
- ⁷Noor, A.K., "Stability of Multilayered Composite Plates," *Fibre Science and Technology*, Vol. 8, 1975, pp. 81-88.
- ⁸Sharma, S., Iyengar, N.G.R., and Murthy, P.N., "Buckling of Antisymmetric Cross- and Angle-Ply Laminated Plates," *International Journal of Mechanical Sciences*, Vol. 22, 1980, pp. 607-620.

Application of Diverging Motions to Calculate Loads for Oscillating Motions

M. H. L. Hounjet*

National Aerospace Laboratory (NLR)
Amsterdam, the Netherlands

Introduction

USUALLY, the unsteady aerodynamic forces needed to calculate flutter are obtained by using the calculation methods for purely harmonic motions. The increased use of active control technology has led to the development of calculation methods that also produce results for nonharmonic motion (exponentially diverging or converging motion).¹

Meanwhile, the technique has become widely accepted to obtain similar results by the analytic continuation of a polynomial fit through aerodynamic loads for purely harmonic motion.² In this way, the accuracy of the approximation is strongly dependent of the accuracy of the aerodynamic loads for harmonic motion. However, for complex configurations, complex flow (transonic), and high frequencies, the accurate calculation of these loads is possible only at relatively high computer costs.

Procedure

In order to reduce these costs, an alternative procedure is used which reflects a suggestion already made by Jones³ in 1945. Consider an arbitrary motion with a time function e^{st} in which the Laplace parameter $s = g + ik$ is complex in general. The procedure includes the following steps:

- 1) Obtain the aerodynamic data for a purely exponentially diverging motion (i.e., g positive and $k = 0$) instead of a harmonic motion as in the usual methods.
- 2) Make a polynomial fit through those data.
- 3) Suppose that the polynomial fit is valid throughout the complex s plane.

The polynomial that is applied is widely used in active control studies is

$$L(s) = \sum_{n=0}^2 a_n s^n + \sum_{n=3}^m a_n \left/ \left(s + \frac{s_{\max}}{n-2} \right) \right.$$

Fitting this polynomial is performed by means of a least squares procedure.

Results

Results obtained with this new approach are presented in Figs. 1-3 for a rectangular wing ($R=2$) that performs a diverging pitching motion about the midchord at a Mach number of 0.8. The wing lift coefficient C_L and moment about the midchord coefficient C_M (both real!) have been calculated with the computer code ARSPNSC developed at NLR. This code is an extension of the ARSPNS code described in Ref. 4 and is capable of treating arbitrary thick lifting and nonlifting bodies oscillating in subsonic flow. Figure 1 shows a comparison of some polynomial fits for a purely diverging ex-

Received Aug. 26, 1985; revision received Jan. 30, 1986. Copyright © American Institute of Aeronautics and Astronautics, Inc., 1986. All rights reserved.

*Senior Research Scientist, Fluid Dynamics Division, Department of Aeroelasticity.